Quantum mechanical methods applied to excitation energy transfer: A comparative analysis on excitation energies and electronic couplings

A. Muñoz-Losa,[1,a)] C. Curutchet,[2,b)] I. Fdez. Galván,[3] and B. Mennucci[1]
[1]*Dipartimento di Chimica e Chimica Industriale, Università degli Studi di Pisa, Via Risorgimento 35, 56126 Pisa, Italy*
[2]*Dipartimento di Chimica Generale ed Inorganica, Chimica Analitica e Chimica Fisica, Università di Parma, Parco Area delle Scienze, I-43100 Parma, Italy*
[3]*Departamento de Ingeniería Química y Química Física, Universidad de Extremadura, Avda. de Elvas s/n, 06071 Badajoz, Spain*

(Received 15 April 2008; accepted 10 June 2008; published online 17 July 2008)

We present a comparative study on the influence of the quantum mechanical (QM) method (including basis set) on the evaluation of transition energies, transition densities and dipoles, and excitation energy transfer (EET) electronic couplings for a series of chromophores (and the corresponding pairs) typically found in organic electro-optical devices and photosynthetic systems. On these systems we have applied five different QM levels of description of increasing accuracy (ZINDO, CIS, TD-DFT, CASSCF, and SAC-CI). In addition, we have tested the effects of a surrounding environment (either mimicking a solvent or a protein matrix) on excitation energies, transition dipoles, and electronic couplings through the polarizable continuum model (PCM) description. Overall, the results obtained suggest that the choice of the QM level of theory affects the electronic couplings much less than it affects excitation energies. We conclude that reasonable estimates can be obtained using moderate basis sets and inexpensive methods such as configuration interaction of single excitations or time-dependent density functional theory when appropriately coupled to realistic solvation models such as PCM. © *2008 American Institute of Physics*. [DOI: 10.1063/1.2953716]

I. INTRODUCTION

The electronic coupling plays a key role in most chemical and biochemical photoinduced energy and electron transfer reactions. In excitation (or resonance) energy transfers (EET) the excitation energy from a donor system in an electronic excited state is transferred to a sensitizer (or acceptor) system. Alternatively, in photoinduced electron transfers, a donor transfers an electron to an acceptor after photoexcitation of one of the components.

One of the most interesting examples where a combination of both these transfer reactions is routinely performed is the photosynthetic process of capturing sunlight with an almost perfect efficiency.[1] In addition, such processes are of fundamental interest in many other fields of science, examples include natural and artificial antennas for the capture and energy conversion of light,[2] amplification of fluorescence-based sensors,[3] optimization of organic light-emitting diodes,[4] and the measurement of structure in biological systems.[5]

Besides this enormous interest in the field and the numerous and important applications involved, the formulation of a computational method able to accurately determine the coupling is still an open problem.[6] If we limit our attention to the EET process only, in most cases large simplifications are introduced as exemplified by the well-known (and largely used) Förster formula.[7] In such model, the EET coupling is assumed to be dominated by the Coulomb interaction, which is approximated using a dipole-dipole model between transition dipole moments of the donor and acceptor systems. In recent years, extraordinary progress has been achieved in the formulation of accurate quantum-mechanical (QM) methods that overcome the limitations of these old models. A significant progress was the development of the so-called "transition density cube" (TDC) method,[8] which calculates numerically the Coulombic interaction between transition densities obtained from *ab initio* methods by representing them in three-dimensional grids or "cubes." Since its first formulation many applications of TDC have been presented in the literature,[9] and its detailed account of the shape of the transition densities has demonstrated the strong limitations of the dipole approximation when chromophores are separated by distances comparable to their molecular dimensions. Another example in the same direction of a more accurate calculation of the coupling is the collective electronic oscillator approach[10] coupled to a semiempirical (INDO/S) description. More recently, a time-dependent density functional theory (TD-DFT) approach has been proposed;[11] as for TDC, transition densities are used to evaluate the coupling but now also exchange and correlation effects can be taken into account. Following a similar strategy, our group has developed a general QM strategy, which allows calculation of the elec-

[a)]Author to whom correspondence should be addressed. Electronic mail: auroraml@ns.dcci.unipi.it.
[b)]Present address: Department of Chemistry, University of Toronto, 80 St. George Street, M5S 3H6 Toronto, Canada.

tronic coupling for systems of increasing complexity including Coulombic, exchange, correlation, and environment effects in a single coherent QM approach.[12] Such a computational strategy avoids numerical problems associated with the three-dimensional grids used in the TDC method, can be used within any QM framework, and has been applied to study inter- (and intra-) molecular EET in molecular systems in liquid solutions, liquid-gas interfaces,[13] as well as in crystal matrices,[14] polymers,[15] and protein environments.[16]

The inclusion of the environment effects is indeed an important issue in the correct estimation of the coupling. As already pointed out by Förster in the formulations of his Coulomb model, the presence of an environment introduces a screening in the donor/acceptor interactions and thus a reduction of the coupling. Such screening effect was introduced by Förster through a scaling factor equal to the inverse of the square of the solvent refractive index $(1/n^2)$.[17]

Recently, we have presented a critical analysis of this factor using our methodology based on the polarizable continuum model (PCM).[18] In such a model, the molecular system under scrutiny (here, the donor-acceptor pair) is described as a QM charge distribution within a molecular cavity of realistic shape, while the environment is described as a structureless polarizable continuum, characterized by its macroscopic dielectric properties. Our methodology captures the key features of the problem, such as an accurate calculation of electronic excited states, the shape of molecules, and the response of the surrounding medium to charge and, importantly, to transition densities. In that analysis we found that, similarly to what is already well known for the Coulomb coupling, the shape of the molecules strongly affects the screening of such couplings, especially at close donor-acceptor separations. We found that the screening of EET interactions is thus far from being a constant factor as proposed by Förster, but it is greatly dependent on the geometrical details (distance, shape, and orientation) of the chromophore pair considered. We also demonstrated that implicit (reaction field) as well as screening effects are dictated mainly by the optical dielectric properties of the host medium, while the effect of the static properties is substantially less important.

Despite all these advances toward appropriate description of the transition densities and environment effects on the calculation of electronic couplings, little attention has been paid to an equally important ingredient in such calculations: the quality of the transition densities. Typically, semiempirical approaches or the configuration interaction of single excitation (CIS) methods have been widely used for such purpose, often along with empirical scaling procedures to correct for the overestimation of transition dipoles predicted by such methods.[18,19] Of course, it would be desirable to avoid such scalings, and recently more accurate QM methods including electron correlation effects are starting to be used to obtain transition densities and compute EET couplings, such as TD-DFT (Ref. 12) or second-order approximate coupled cluster (CC2).[20]

Given all these developments in the field, it becomes important to analyze in more detail both the accuracy and the reliability of the QM methods proposed to evaluate the coupling using different levels of theory and different basis sets. Such an analysis has been largely applied to excitation energies especially in the last years since the explosion of TD-DFT methods to study absorption and emission spectra of molecular systems. By contrast, much less is known about the effects of the QM description on the electronic coupling. In this paper, we present a comparative study based on the computational approach we have developed to study EET for molecular systems eventually embedded in a polarizable environment. In order to have a more complete picture, two different families of systems have been analyzed, namely, two examples of chromophores present in many organic electro-optical devices based on EET processes (naphthalene and perylene dimers) and two examples of chromophores (bilins and chlorophylls) taken from photosynthetic light-harvesting antenna proteins.

Several model dyads based on naphthalene[12(b),21–24] and perylene chromophoric units[15,20,25] have been specifically designed and used to study EET mechanisms, both theoretically and experimentally. It is therefore particularly interesting to compare different QM approaches in the calculation of electronic couplings for these systems. On the other hand, the bilin and chlorophyll pairs represent two different examples of strongly coupled chromophores that can be found in photosynthetic antenna proteins. In particular, we have selected the central phycoerythrobilin (PEB) pair of the phycoerythrin 545 (PE545) light-harvesting antennae from the cryptophyte alga *Rhodomonas* CS24 (Ref. 26) and the bacteriochlorophyll *a*–bacteriopheophytin *a* (B-H) pair of the reaction center (RC) of the purple photosynthetic bacterium *Rhodobacter sphaeroides*.[27] This choice has been suggested by the chance to have a direct comparison with the experimental estimation of their electronic coupling recently obtained using one- and two-color, three-pulse photon echo peak shift spectroscopy.[28]

On these four different systems we have applied five different QM levels of description: Zerner's intermediate neglect of differential overlap (ZINDO),[29] CIS,[30] TD-DFT,[31] symmetry-adapted cluster/configuration interaction (SAC-CI),[32] and complete-active-space self-consistent field (CASSCF);[33] in the latter case perturbative corrections have been introduced where possible using a complete-active-space second-order perturbative approach (CASPT2).[34]

To have a clearer picture, two separate analyses of the results are reported in Sec. III. The first is on excitation energies and the corresponding transition dipoles, whereas the second is on the electronic coupling; in both cases the environment effects are also analyzed. The two analyses are preceded by a short description of the methods used (Sec. II) and concluded by a summary (Sec. IV).

II. METHODS

To analyze and compare the relative sensitivity of excitation energies and electronic coupling on the QM level of description, we have selected five representative approaches, the most largely used linear response (LR) approaches, based either on semiempirical, Hartree–Fock or DFT description of the reference state (ZINDO, CIS, and TD-DFT, respectively)

and two more refined approaches to treat excited states, SAC-CI and CASSCF (and CASPT2). With respect to the first three, the main difference is that these two methods overcome the limitation of using only single excitations, and with respect to ZINDO and CIS, they also take into account correlation effects. For all these reasons SAC-CI and CASSCF results will represent a kind of benchmark for our calculations (together with experimental data if available).

All calculations of the coupling in gas phase and including the environment have been performed using a locally modified version of the GAUSSIAN package, in which we have implemented our QM model for the EET coupling.

The most general formulation of such a model, which is described in detail in Ref. 12, evaluates the coupling applying a QM LR approach in which the effect of a polarizable environment is taken into account using a PCM description. In particular, an approximate solution of the LR scheme is introduced in which the donor-acceptor (D/A) interaction is considered as a perturbation, and the electronic coupling is obtained from the transition densities of the isolated chromophores in the absence of their interaction. To first order, the electronic coupling V is obtained as a sum of two terms, the direct contribution (implicitly modified by the environment) V_s and the contribution involving the explicit environment effect, V_{explicit},

$$V = V_s(\rho_D^T, \rho_A^T) + V_{\text{explicit}}(\rho_D^T, \rho_A^T; \varepsilon_{\text{opt}}),$$

$$V_s(\rho_D^T, \rho_A^T) = \int d\mathbf{r} \int d\mathbf{r}' \rho_A^{T*}(\mathbf{r}') \left(\frac{1}{|\mathbf{r}' - \mathbf{r}|} + g_{\text{xc}}(\mathbf{r}', \mathbf{r}) \right) \rho_D^T(\mathbf{r}) - \omega_0 \int d\mathbf{r} \int d\mathbf{r}' \rho_A^{T*}(\mathbf{r}') \rho_D^T(\mathbf{r}), \quad (1)$$

$$V_{\text{explicit}}(\rho_D^T, \rho_A^T; \varepsilon_{\text{opt}}) = \sum_k \left(\int \rho_A^{T*}(\mathbf{r}) \frac{1}{|\mathbf{r} - \mathbf{s}_k|} \right) q(\mathbf{s}_k; \rho_D^T, \varepsilon_{\text{opt}}),$$

where $\rho_{D/A}^T$ indicates the transition densities of the donor (the acceptor) in the absence of their interactions, ω_0 their common transition energy, and $g_{\text{xc}}(\mathbf{r}', \mathbf{r})$ is the exchange plus correlation kernel, $\mathbf{r}$ being the electronic coordinate.

As it can be seen from the second equation, the direct contribution (V_s) contains different terms depending on the QM level of theory chosen, namely, Coulombic and overlap in all cases, plus exchange and correlation (defined in terms of the g_{xc} kernel). The explicit contribution of the environment to the coupling (V_{explicit}) is computed by describing the permittivity-dependent polarization induced by the solute on the environment—the reaction field—as a set of apparent surface charges (q) distributed on the surface of the molecular-shaped cavity containing the solute. In particular, a nonequilibrium response for the environment (indicated by the dynamic or optical part of the permittivity ε_{opt}) is assumed in the EET process. Obviously, V_{explicit} disappears when gas-phase D/A pairs are considered, in those cases also the transition densities refer to isolated systems. A useful way to analyze the environment effects, which will be used in the next section, is in terms of the scaling function s introduced in Ref. 16; this is defined as

$$s = \frac{V_s + V_{\text{explicit}}}{V_s} \quad (2)$$

and can be directly compared to the Förster screening factor $(1/n^2)$ (here n^2, the square of the refractive index, approximates ε_{opt}).

As said, to describe the effects of the environment the PCM has been used. In such a model the only parameters needed are the positions and radii of the spheres determining the cavity embedding the D/A pair and the environment optical $(\varepsilon_{\text{opt}})$ and static (ε_0) permittivities. In order to compare our results to available experimental data, we have used both ε_{opt} and ε_0 values equal to 1.88 to describe *n*-hexane and $\varepsilon_{\text{opt}}=2.232$ and $\varepsilon_0=2.379$ to simulate toluene. Both solvents resemble typical apolar environments embedding chromophores in organic devices. To describe the dielectric properties of the proteins we have selected the values of 2 for ε_{opt} and 15 for ε_0. These values have been obtained from dielectric dispersion measurements on hydrated lysozyme powders, and in Ref. 35 it has been shown that these values describe well solvation dynamics of protein environments. Indeed $\varepsilon_{\text{opt}}=2$ is a commonly accepted value for different kinds of proteins, while the static ε_0 is known to depend on the specific protein or even on the specific region inside a particular protein.[16] PCM cavities have been constructed from radii obtained by applying the united atom topological model to the atomic radii of the UFF (Ref. 36) force field as implemented in the GAUSSIAN 03 code.[37] Transition energies and solvent shifts discussed on Sec. III A have been obtained using cavities corresponding to single monomers. However, transition densities and couplings discussed in Sec. III B have been obtained by considering the cavity enclosing the chromophore D/A pair.

Geometries were obtained as follows. For naphthalene and perylene, single chromophore properties discussed in Sec. III A were obtained on a geometry optimized at the B3LYP/6-31G(*d*) level. Electronic couplings for the naphthalene dimer were obtained adopting the orientation of the naphthalene units as found in the DN4 naphthalene bridged dimer.[12(b)] This was accomplished by simply eliminating bridge atoms on the DN4 B3LYP/6-31G(*d*,*p*) optimized geometry and then introducing hydrogens at standard bond lengths to saturate valences of the appropriate carbon atoms. For perylene, couplings were computed by using the crystal structure reported in Ref. 38. For chlorophyll and bilin systems, all calculations were performed on the geometries obtained from published structural models, where hydrogens were added and optimized at the HF/6-31G level keeping all of the other atoms frozen. The crystal structure of the phycoerythrin 545 (PE545) light-harvesting antennas from the cryptophyte algae *Rhodomonas* CS24 was determined at an ultrahigh resolution of up to 0.97 Å (Ref. 26) and corresponds to the 1XG0 entry in the Protein Data Bank, while the structure of the RC of the purple photosynthetic bacterium *Rhodobacter sphaeroides*[27] was determined at 2.65 Å resolution (1PCR entry).

In the multiconfigurational calculations different active spaces were selected according to the size of the system. For the naphthalene molecule the complete active π space was

introduced in the calculations, i.e., ten electrons and ten orbitals. In the other systems it is not viable to introduce the complete active π space, so $8e/8o$ active space was chosen for the perylene, PEB, BCL *a*, and BPH *a* molecules. The energies of the different states are calculated using the state-averaged method for the ground and the excited states, a total of ten states were considered for the naphthalene, two states for perylene and bilin, and three states for chlorophyll. The perturbation selection of the double excitation operators for SAC-CI SD-R calculations was carried out with energy thresholds of 5×10^{-6} and 5×10^{-7} a.u. for the ground and excited states, respectively. Excitations from core orbitals were excluded in all QM calculations except for ZINDO. All TD-DFT calculations were performed using the hybrid B3LYP exchange-correlation functional.

ZINDO, CIS, TD-DFT, and SAC-CI energies and transition properties (dipoles and densities to be used in the coupling calculations) have been calculated with the standard GAUSSIAN 03 package,[37] whereas the CASSCF energies (including the CASPT2 correction) and transition dipoles and densities have been calculated using MOLCAS 6.4.[39] CASSCF transition densities have been stored on a file and read by the modified version of Gaussian to calculate the coupling.

III. RESULTS

A. Excitation energies and transition dipoles

Before presenting the EET couplings of the four optically active systems we report the analysis of the involved electronic transitions in vacuum and in condensed phase. The influence of different QM methods and basis sets in excitation energies, solvent or protein shifts, and transition dipoles will be discussed for each chromophore.

1. Naphthalene

The experimental absorption spectrum of naphthalene in gas phase[40] is characterized by an intense band placed at 5.89 eV, which is identified as a π-π^* electronic transition with $^2B_{2u}$ symmetry, and two other weak bands placed at 4.45 and 3.97 eV that correspond to π-π^* transitions with $^1B_{1u}$ and $^1B_{2u}$ symmetries, respectively. A slight redshift of the bands is observed when the system is studied in *n*-hexane solution.[41] Since *n*-hexane is an apolar solvent, a small redshift of ~0.3 eV is observed for the allowed transition and almost negligible ones for the weakly allowed transitions. These three bands are identified in the spectrum in *n*-hexane at 5.62, 4.34, and 3.94 eV, respectively, with similar oscillator strengths to those in the gas-phase spectrum. The naphthalene excitation energies, transition dipoles, and solvent shifts calculated at different QM levels of theory are collected in Table I.

As found in a previous study,[12(b)] the ZINDO method underestimates the electronic transition energies of the states with B_{2u} symmetry, but it reproduces well the values of the redshifts. On the other hand, the energies obtained with CIS are clearly overestimated both in vacuum and in *n*-hexane solution. On the contrary, the TD-B3LYP method provides results in good agreement with the experimental data except for the $^1B_{2u}$ state, which is somewhat overestimated, this fact leading to an exchange in the order of the two lowest lying transitions.

Moving to the SAC-CI results, we can note that although this is a high-level method that introduces single and double excitations in the QM calculation, a notable overestimation of the excitation energies of ~0.4–1.0 eV is obtained for all three states. Similar overestimations were found in previous studies of benzene using this method[42] and also for these states of naphthalene using the comparable second-order approximate coupled cluster (CC2).[43] The use of the SD-R version of SAC-CI, thus neglecting higher order excitations, and the use of a relatively small basis set could explain the disagreement between SAC-CI energies and experiment.

Multiconfigurational methods are well-known methods in the theoretical study of optical properties. However, as the CASSCF method only introduces the static electronic correlation component in the calculation of the electronic transition energies, it is not surprising that these energies are strongly overestimated as we can observe in Table I (a disagreement of more than 2 eV is found for the allowed transition). In systems with a highly resonant π electronic structure, as in this case, it is, in fact, necessary to introduce the dynamic electron correlation in order to obtain accurate excitation energies. This is illustrated by the CASPT2 results, which show a much better agreement with experiments. In the CASPT2 calculations, we can see how the introduction of polarization functions, passing from the 6-31G to the 6-31G(*d*) basis set, greatly improves the agreement with experiment, these latter results being similar to those obtained with the Dunning cc-pVDZ basis set. The transition energy overestimation obtained for the more extended basis set is also found in previous studies.[43]

When we move to consider solvent effects, we note that in contrast to what was found for the absolute transition energies, solvent shifts are quite independent of the basis set used while they show a not negligible dependency on the QM method. In particular, ZINDO and CIS shifts are very similar but they are both larger than TD-B3LYP values especially for the intense π-π^* electronic transition with $^2B_{2u}$ symmetry. In all cases, however, the calculated values reproduce the experimental redshifts of 0.03, 0.11, and 0.27 eV, for $^1B_{2u}$, $^1B_{1u}$, and $^2B_{2u}$ states, respectively.

Finally, in the present framework, it is important to comment on transition dipoles and their dependence on both basis set and QM methods. Beginning from the most complete methods, we note the SAC-CI and CASSCF/CASPT2 methods give very similar results, and, in general, little variation with respect to the basis set is found. If we consider these latter as our benchmark, we find that TD-B3LYP underestimates by ~10% the transition dipole, while the CIS and ZINDO methods overestimate it by ~10%.

2. Perylene diimide

In the perylene diimide (PDI), the study has been focused on the lowest allowed $\pi\rightarrow\pi^*$ electronic transition; this is characterized by a highest occupied molecular orbital–

TABLE I. Transition energies, in vacuum, and solvent shifts (in *n*-hexane) calculated for the $^1B_{2u}$, $^1B_{1u}$, and $^2B_{2u}$ states of naphthalene. Transition dipole moments and their variation upon solvation correspond to the brightest $^2B_{2u}$ state. Energies and dipole moments are in eV and Debye, respectively.

		ΔE			**δ**				
		$^1B_{2u}$	$^1B_{1u}$	$^2B_{2u}$	$^1B_{2u}$	$^1B_{1u}$	$^2B_{2u}$	$\boldsymbol{\mu}^T$	$\boldsymbol{\Delta\mu}^T$
ZINDO		3.91	4.16	5.25	0.00	−0.06	−0.31	9.1	0.4
CIS									
	6-31G	5.45	5.35	7.42	0.00	−0.07	−0.36	9.3	0.6
	6-31G(*d*)	5.33	5.21	7.30	0.00	−0.06	−0.36	9.3	0.6
	cc-pVDZ	5.25	5.12	7.20	0.00	−0.05	−0.37	9.4	0.6
	6-31+G(*d*)	5.21	5.08	6.88	0.00	−0.06	−0.33	9.1	0.8
TD-B3LYP									
	6-31G	4.57	4.54	6.18	0.00	−0.03	−0.23	7.3	0.7
	6-31G(*d*)	4.50	4.43	6.08	0.00	−0.03	−0.23	7.2	0.8
	cc-pVDZ	4.46	4.38	6.01	0.00	−0.03	−0.23	7.3	0.8
	6-31+G(*d*)	4.43	4.35	5.83	0.00	−0.04	−0.23	7.5	0.8
SAC-CI									
	6-31G	4.22	5.36	6.87				8.1	
	6-31G(*d*)	4.18	5.10	6.74				8.2	
	cc-pVDZ	4.17	4.99	6.67				8.3	
	6-31+G(*d*)	4.41	5.08	6.55				8.3	
CASSCF									
	6-31G	4.14	6.78	8.30				7.9	
	6-31G(*d*)	4.11	6.53	8.15				8.0	
	cc-pVDZ	4.10	6.42	8.06				8.1	
	6-31+G(*d*)	4.09	6.42	8.02				8.1	
CASPT2									
	6-31G	4.16	5.05	6.19				7.9	
	6-31G(*d*)	4.00	4.59	5.76				8.0	
	cc-pVDZ	3.97	4.41	5.88				8.1	
	6-31+G(*d*)	4.31	4.74	6.06				8.1	
Exp.[a]		3.97	4.45	5.89	−0.03	−0.11	−0.27		

[a]References 40 and 41.

lowest unoccupied molecular orbital contribution and it has $^1B_{2u}$ symmetry. To our knowledge, no gas-phase spectra have been obtained experimentally, while in toluene solution this band is found at ~2.36 eV for Ph-PDI-Ph.[25,44] The results in transition energies, dipoles, and solvent shifts obtained by using different QM methods and basis sets for PDI are shown in Table II.

As expected, the CIS method overestimates by more than 30% the electronic transition energy. However, in contrast to what was found in the naphthalene system, the ZINDO method provides a good result in toluene. Also TD-B3LYP seems to be a valid method for this system, since, independently of the basis set, the excitation energies are in very good agreement with experiments. These results are similar to what was found in previous TD-B3LYP calculations on PDI.[15]

Exploiting the fact that in an apolar solvent such as toluene, the solvent shift is small, and the effects of changing the QM method are small too, we can compare the SAC-CI or CASSCF results to the experimental estimate in toluene. As a matter of fact, small redshifts are obtained using either ZINDO, CIS, or TD-B3LYP method; in all cases the shift is around 0.1–0.2 eV. Assuming that this solvent shift is also valid for the other methods, we find that SAC-CI slightly overestimates the observed energy, although to a much lesser extent than for naphthalene; with the 6-31G(*d*) basis set, the error is only of ~0.1–0.2 eV. Depending on the basis set, SAC-CI energies are larger than TD-B3LYP results by ~0.1–0.3 eV, this difference being similar to what was found between the similar CC2 method and TD-B3LYP for PDI in a recent study.[20]

Finally, the comparison between CASSCF and CASPT2 results shows once more the importance of introducing the dynamic electronic correlation to obtain accurate energies. Using a 0.1–0.2 eV solvent shift, we find that the CASPT2 method slightly underestimates the transition energy by about 0.2–0.3 eV for the 6-31G(*d*) basis set, while with the 6-31G one it gives results in very good agreement with experiment.

In the same line to what was observed for naphthalene, for PDI we obtain very similar transition dipole moments at SAC-CI and CASSCF levels. In this case, however, the TD-B3LYP method gives similar dipoles only underestimated by ~3%–5%, while, once again, CIS and ZINDO overestimate these values by ~10%. In addition, the SAC-CI, CASSCF, and TD-B3LYP estimates are in agreement with the result obtained at the CC2/SVP level (8.65 D) by Fückel *et al.*[20]

TABLE II. Transition energies and dipoles, in vacuum, and the corresponding shifts in toluene solution calculated for the $^1B_{2u}$ state of PDI. Energies and dipole moments are in eV and Debye, respectively.

		ΔE	δ	μ^T	$\Delta\mu^T$
ZINDO		2.71	−0.21	10.6	1.1
CIS					
	6-31G	3.50	−0.17	10.0	0.8
	6-31G(*d*)	3.46	−0.16	9.7	0.9
	cc-pVDZ	3.42	−0.16	9.6	0.8
	6-31+G(*d*)	3.36	−0.16	9.6	0.9
TD-B3LYP					
	6-31G	2.56	−0.13	8.6	1.3
	6-31G(*d*)	2.52	−0.12	8.4	1.3
	cc-pVDZ	2.50	−0.12	8.3	1.3
	6-31+G(*d*)	2.45	−0.13	8.5	1.4
SAC-CI					
	6-31G	2.87		9.1	
	6-31G(*d*)	2.66		8.9	
CASSCF					
	6-31G	4.59		8.9	
	6-31G(*d*)	4.53		8.8	
CASPT2					
	6-31G	2.51		8.9	
	6-31G(*d*)	2.27		8.8	

We can thus conclude that the basis set does not have an important influence in the evaluation of the transition dipole, and that the differences found between the various QM methods, both regarding the transition energies and dipoles, are smaller than in the naphthalene study.

3. PEB

The phycoerythrin 545 protein is the primary light-harvesting antenna from the cryptophyte alga *Rhodomonas* CS24. Phycobiliproteins are particular antenna systems that allow efficient capture of light in aquatic environments where the available spectral window and quantity of light is reduced. Although the absorption spectrum of the PE545 protein is built from excitonic states to which the eight bilin chromophores of the protein can contribute, previous theoretical calculations on this system suggest that the transition energy of the two central PEB pigments is located on the high-energy side of the protein observed band, so it is expected to be around 2.2–2.3 eV.[45] We have chosen the central PEB pair in this work as these are the most strongly coupled pigments in PE545, so we can expect a higher sensitivity of the electronic coupling with respect to the QM description adopted in this case.

In Table III we show the results obtained for the PEB pair, in this case, in fact, the two chromophores are not equivalent due to structural differences induced by their position within the protein.

As found for the PDI system, also for PEB the ZINDO method provides a transition energy in good agreement with the experiments. In contrast, CIS calculations strongly overestimate the energy by about 1 eV, while TD-B3LYP values are larger than experiment by about 0.3–0.4 eV. To better appreciate the TD-B3LYP results, we note that an unexpected electronic state lying below our state of interest is found; this shows a partial charge-transfer character. The variable degree of mixing of these states induces some instability on the estimate of both transition energies and dipoles with respect to the basis set, which we do not observe in any other system or for any other QM method used in the present study. The overstabilization of charge-transfer states by TD-B3LYP is a well-known deficiency of present exchange-correlation functionals,[46] the present results of PEB chromophores seem to confirm this behavior: as a result the variations on the transition dipoles as a function of the basis set should also be regarded as an artifact of the TD-B3LYP method for this system.

Regarding the protein redshifts, either with ZINDO, CIS, or TD-B3LYP we find that solvation lowers the transition energies by about 0.2 eV except for some TD-B3LYP calculations on the PEB 50/61C molecule, in which the shift is sensibly smaller. However, this latter discrepancy could be due to the problems encountered with TD-B3LYP for these systems, as previously discussed. If we assume a similar shift of ~0.2 eV for the vacuum SAC-CI and CASSCF energies, we find that SAC-CI overestimates experiment by about 0.5 eV, while not surprisingly CASSCF gives much higher values. Regarding the CASSCF energies, however, the most notable result is the large energy difference found between the two chromophores, in clear contradiction to what was found for all the other methods. For this pair we do not report CASPT2 calculations because of the high computational cost this would involve.

Here we want to note that, beside the quality of the geometry used in the calculations, it is also possible that the

TABLE III. Transition energies and dipoles, in vacuum, and the corresponding shifts in the protein environment, calculated for the first excited state of the PEB 50/61D and PEB 50/61C chromophores. Energies and dipole moments are in eV and Debye, respectively.

		ΔE	δ	μ^T	$\Delta\mu^T$
ZINDO		2.46/2.40	−0.24/−0.26	11.2/12.1	0.4/0.2
CIS					
	6-31G	3.52/3.44	−0.21/−0.19	11.5/12.2	0.4/0.4
	6-31G(*d*)	3.46/3.38	−0.21/−0.20	11.4/12.2	0.4/0.4
	cc-pVDZ	3.43/3.35	−0.20/−0.19	11.4/12.2	0.5/0.4
	6-31+G(*d*)	3.39/3.31	−0.20/−0.19	11.3/11.7	0.4/0.4
TD-B3LYP					
	6-31G	2.88/2.84	−0.11/−0.05	8.2/8.9	1.2/−1.1
	6-31G(*d*)	2.87/2.82	−0.14/−0.05	10.3/9.2	−0.7/−1.3
	cc-pVDZ	2.85/2.80	−0.14/−0.06	10.3/9.3	−0.7/−1.4
	6-31+G(*d*)	2.81/2.76	−0.16/−0.24	10.4/9.0	0.3/0.5
SAC-CI					
	6-31G	2.92/2.85		9.9/10.5	
CASSCF					
	6-31G	3.87/3.51		9.6/10.4	

overestimation of experimental transition energies by SAC-CI and TD-B3LYP methods is due to the fact that these chromophores are protonated in the protein matrix. In a recent theoretical study on a similar phytochromobilin molecule published by Borg and Durbeej[47] similar results were obtained between TD-B3LYP and SAC-CI for the neutral pigment, while consideration of the protonated system lowered the transition energies by 0.4–0.6 and 0.1–0.2 eV for SAC-CI and TD-B3LYP, respectively, the SAC-CI results being in good agreement with experiment. Similar shifts due to protonation of the phytochromobilin at the SAC-CI level were found in another study.[48] In the present paper, however, we want to focus in the comparison of different QM methods rather than to experiment and analyze how this affects the estimation of the electronic coupling. So, a more detailed study of the protonation state of the PEB pigments is out of the scope of this paper. In addition, we note that the protein shifts we obtain are similar to those found in other studies for similar bilin pigments.[47,49,50]

Finally, as for naphthalene and PDI, also for the bilins we find a very good agreement between transition dipoles obtained from CASSCF and SAC-CI calculations. Also, we find that CIS and ZINDO methods overestimate these values by more than 10%. Regarding the TD-B3LYP results, the instability induced by the degree of mixing of the above-mentioned artificial low-lying state with our state of interest induces large variations in the dipoles between basis sets, and also when passing from vacuum to condensed phase, in some cases solvation inducing an enhancement and in others a reduction of the dipole magnitudes. This shows that TD-B3LYP methods have to be used with particular care regarding the computation of transition dipoles in cases where such kind of mixings occur, as dipoles seem to be much more affected by this kind of instability than the transition energies.

4. Bacteriochlorophyll/bacteriopheophytin

The bacteriochlorophyll (BCL) and bacteriopheophytin (BPH) pigments we consider here are found in the RC of purple photosynthetic bacteria, which is formed by six chromophores: a BCL, an accessory BCL, and a BPH in each of the A and B sides of RC. A recent experimental study by Fleming *et al.*[51] provides the absorption spectrum of the RC of *Rhodobacter sphaeroides*, showing three main bands labeled H, B, and P, and centered at ~750 nm (1.65 eV), ~800 nm (1.55 eV), and ~860 nm (1.44 eV), respectively. The labeling denotes which chromophore mostly contributes to each band, although each band has contributions from multiple chromophores because these are electronically coupled and is also the superposition of the chromophores in the A and B sides. Here we will adopt the experimental values for the B and H bands as the approximate value for the transition energies of the BCL and BPH pigments, respectively. In Table IV the results for the two systems are reported.

Except for the multiconfigurational CASSCF method, all the other QM methods reproduce the correct order for the B and H bands. However, the energetic difference between H and B, which is around 0.1 eV (see Table IV), is overestimated by ZINDO and CIS calculations, which give differences of 0.2 and ~0.3 eV, respectively. In contrast, TD-B3LYP results accurately reproduce the experimental difference. In addition, this difference is quite similar in gas phase and in solution, given that we obtain very similar protein shifts for the two pigments, while for ZINDO and CIS a notable larger shift is obtained for the BCL chromophore. Assuming valid protein shifts for BCL and BPH found at TD-B3LYP level, i.e., similar for both chromophores, SAC-CI values adequately reproduce the experimental energy difference. We note that for this system, CIS values are closer to the experimental data than TD-B3LYP.

Regarding the absolute values, the ZINDO method

TABLE IV. Transition energies and dipoles, in vacuum, and the corresponding shifts in the protein environment, calculated for the first excited state (Q_y) of the BCL and BPH chromophores. Energies and dipole moments are in eV and Debye, respectively.

		ΔE		δ		μ^T		$\Delta\mu^T$	
		BCL	BPH	BCL	BPH	BCL	BPH	BCL	BPH
ZINDO		1.22	1.27	−0.19	−0.04	11.4	9.5	1.5	1.1
CIS									
	6-31G	1.85	2.03	−0.16	−0.04	9.8	8.1	1.3	1.3
	6-31G(*d*)	1.75	1.98	−0.08	0.02	9.9	8.5	1.1	1.1
	cc-pVDZ	1.73	1.97	−0.06	0.04	9.9	8.5	1.0	1.1
	6-31+G(*d*)	1.70	1.94	−0.05	0.04	10.0	8.6	1.1	1.1
TD-B3LYP									
	6-31G	1.87	1.97	−0.10	−0.09	7.0	6.0	1.5	1.3
	6-31G(*d*)	1.81	1.93	−0.09	−0.09	7.0	6.1	1.4	1.4
	cc-pVDZ	1.80	1.92	−0.09	−0.08	7.0	6.1	1.4	1.4
	6-31+G(*d*)	1.77	1.88	−0.10	−0.09	7.2	6.0	1.6	1.8
SAC-CI									
	6-31G	1.58	1.62			9.1	7.5		
CASSCF									
	6-31G	2.44	2.27			7.7	6.7		

strongly underestimates the excitation energy of the two molecules. The CIS method improves considerably the description since it correctly assigns the B band (~0.1 eV error) and the H band is only overestimated by ~0.3 eV. On the other hand, the TD-B3LYP method gives results in very good agreement with experiment. Finally, SAC-CI energies, assuming a similar ~0.1 eV protein shift for both chromophores, lead to excellent agreement with experiment. We note that Hasegawa and Nakatsuji[52] used the SAC-CI method to study the excited states of the photosynthetic RC of the *Rhodobacter sphaeroides* and assigned the H_a and B_a electronic bands at 1.86 and 1.48 eV, respectively. The differences in the excitation energy with respect to our results can be ascribed not only to the use of different molecular geometries and basis sets but also to the use of a less accurate threshold for the selection of double excitations in that study.

Passing to the CASSCF results, and assuming a ~0.1 eV protein shift as for SAC-CI, we observe that the energies are overestimated for both B and H transitions. Again this is not surprising and is due to the neglect of dynamic electron correlation. The reason for the exchange in position of the B and H electronic bands in the CASSCF calculations could be the use of a poor basis set (especially for a molecule that includes a metal such as BCL), and of a small active space. Here, in fact, we used eight electrons in eight orbitals, whereas a previous study by Rubio *et al.*[53] on a similar molecule employed a larger active space of 18 electrons in 15 orbitals. As for the PEB pair, here we have not performed CASPT2 calculations because of their high computational cost.

Regarding the transition dipole moments, we observe that, as before, also here CIS and ZINDO give much larger values compared to TD-B3LYP, SAC-CI, or CASSCF. However, in contrast to what we found for the other systems, we find a strong variation of the transition dipoles with the QM approach. In particular, for this system we find that CASSCF and TD-B3LYP values are 10%–15% and 20% lower than SAC-CI estimates, respectively, while CIS and ZINDO are increased by 10%–15% and 25% with respect to SAC-CI.

B. Electronic coupling

In the previous section, we have shown that the transition energies predicted for various typical chromophoric units are strongly dependent on the QM methodology, giving rise to differences as large as 1–2 eV in some cases. In addition, the particular choice of basis set can further shift these estimates over several tenths of eV, depending on the particular system and QM method under consideration. However, transition dipole moments show a less pronounced dependency over the QM method, and interestingly very small differences arise as a consequence of the basis set choice. In the present section we will turn our attention to the effects that these factors have on the estimation of the electronic coupling.

In Tables V–VIII we report, for each pair, the electronic couplings calculated in vacuum using the ZINDO, CIS, TD-B3LYP, SAC-CI, and CASSCF transition densities obtained by using different basis sets.

For the semiempirical ZINDO method, only the Coulomb term is shown as exchange and overlap contributions are zero by definition. For the other methods, we dissect the coupling into Coulomb, exchange, and overlap contributions, and a further exchange-correlation term is obtained when using TD-B3LYP. We also include the electronic coupling obtained from the point dipole approximation (PDA) using the transition dipoles obtained from the corresponding QM calculations, as this will help us in correlating the changes in the transition dipoles with those found on the electronic cou-

TABLE V. Naphthalene dimer in vacuum: Coulomb, Hartree–Fock exchange, exchange-correlation, and overlap contributions to the total electronic coupling V along with the estimates obtained from the PDA $V^{\text{dip-dip}}$ Separation between the charge centers of 8.3 Å. All values are in cm^{-1}.

		$\mathbf{V}^{\text{Coul}}$	$\mathbf{V}^{\text{hfx}}$	$\mathbf{V}^{\text{xc}}$	$\mathbf{V}^{\text{ovlp}}$	$\mathbf{V}$	$\mathbf{V}^{\text{dip-dip}}$
ZINDO		679.4				679.4	1088.8
CIS							
	6-31G	1201.7	−0.2		0.0	1201.5	1131.1
	6-31(*d*)	1187.8	−0.2		0.0	1187.6	1118.5
	cc-pVDZ	1221.3	−0.7		−4.0	1216.6	1146.1
	6-31G(*d*)	1140.0	−59.2		0.3	1081.0	1014.1
TD-B3LYP							
	6-31G	712.3	0.0	0.1	0.0	712.4	692.8
	6-31G(*d*)	699.8	0.0	0.1	0.0	699.9	681.3
	cc-pVDZ	721.6	−0.1	0.1	−0.2	721.4	701.1
	6-31G(*d*)	774.4	−4.2	−6.3	0.1	764.0	742.8
SAC-CI							
	6-31G	913.9	−0.1		0.0	913.8	874.3
	6-31G(*d*)	918.5	−0.1		0.0	918.5	879.4
	cc-pVDZ	973.9	−0.2		−0.7	973.0	930.9
	6-31G(*d*)	975.9	−17.6		0.0	958.3	922.5
CASSCF							
	6-31G	884.8	0.0		0.0	884.8	831.4
	6-31G(*d*)	885.6	0.0		0.0	885.6	842.9
	cc-pVDZ	910.0	−0.1		7.0	917.0	852.5
	6-31G(*d*)	911.1	−1.2		0.0	909.9	861.2

pling. In Förster model, the coupling is approximated as the product of the PDA coupling, $V^{\text{dip-dip}}$, and a solvent screening factor $1/n^2$,

$$V = sV_s \approx \frac{1}{n^2} V^{\text{dip-dip}} = \frac{1}{n^2} \frac{k\mu_D^T \mu_A^T}{R^3}, \tag{3}$$

where μ_D^T/μ_A^T are the D/A transition dipole moments, R the center-to-center separation, and k the orientation factor $[k=\hat{\mu}_D^T \cdot \hat{\mu}_A^T - 3(\hat{\mu}_D^T \cdot \hat{R})(\hat{\mu}_A^T \cdot \hat{R})$, where $\hat{\mu}_D^T$, $\hat{\mu}_A^T$ and $\hat{R}$ are unit vectors].

The structures of the four chromophore pairs are reported in Fig. 1; for all of them we can define an interpigment distance using the center of charge of the transition densities: the resulting distances are 8.3, 3.9, 17.1, and 11.3 Å, for the naphthalene, perylene, and PEB, dimers, and the BCL-BPH pair, respectively.

TABLE VI. PDI dimer in vacuum: Coulomb, Hartree–Fock exchange, exchange-correlation, and overlap contributions to the total electronic coupling V along with the estimates obtained from the PDA $V^{\text{dip-dip}}$. Separation between the charge centers of 3.9 Å. All values are in cm^{-1}.

		$\mathbf{V}^{\text{Coul}}$	$\mathbf{V}^{\text{hfx}}$	$\mathbf{V}^{\text{xc}}$	$\mathbf{V}^{\text{ovlp}}$	$\mathbf{V}$	$\mathbf{V}^{\text{dip-dip}}$
ZINDO		1243.0				1243.0	8034.9
CIS							
	6-31G	1506.9	15.1		−0.1	1522.0	7146.0
	6-31G(*d*)	1438.3	14.4		−0.1	1452.6	6738.0
	cc-pVDZ	1406.0	19.3		−12.6	1412.7	6565.0
	6-31+G(*d*)	1398.3	12.2		0.0	1410.6	6598.3
TD-B3LYP							
	6-31G	1024.2	0.4	0.0	0.0	1024.6	5250.3
	6-31G(*d*)	978.1	0.3	0.0	0.0	978.4	5001.4
	cc-pVDZ	959.0	0.4	−0.2	0.0	959.2	4898.7
	6-31+G(*d*)	991.8	−0.9	−2.2	0.0	988.7	5154.0
SAC-CI							
	6-31G	1318.5	3.4		0.0	1321.9	5947.7
	6-31G(*d*)	1267.4	3.0		0.0	1270.4	5631.8
CASSCF							
	6-31G	1633.6	2.3		0.0	1635.9	4924.0
	6-31G(*d*)	1552.8	8.2		0.0	1561.0	4856.1

TABLE VII. PEB 50/61D-PEB 50/61C dimer in vacuum: Coulomb, Hartree–Fock exchange, exchange-correlation, and overlap contributions to the total electronic coupling V along with the estimates obtained from the PDA $V^{\text{dip-dip}}$. Separation between the charge centers of 17.1 Å. All values are in cm^{-1}.

		$\mathbf{V}^{\text{Coul}}$	$\mathbf{V}^{\text{hfx}}$	$\mathbf{V}^{\text{xc}}$	$\mathbf{V}^{\text{ovlp}}$	$\mathbf{V}$	$\mathbf{V}^{\text{dip-dip}}$
ZINDO		131.8				131.8	96.3
CIS							
	6-31G	169.2	−0.1		0.0	169.1	92.8
	6-31G(*d*)	166.3	−0.1		0.0	166.2	91.5
	cc-pVDZ	166.2	−0.2		−1.6	164.4	91.3
	6-31+G(*d*)	165.9	−0.4		0.0	165.5	90.3
TD-B3LYP							
	6-31G	129.3	0.0	−0.1	0.0	129.2	62.4
	6-31G(*d*)	167.0	−0.1	−0.1	0.0	166.8	81.5
	cc-pVDZ	168.3	−0.1	0.1	0.1	168.4	82.1
	6-31+G(*d*)	166.1	−0.2	−0.2	0.0	165.7	81.2
SAC-CI							
	6-31G	134.9	−0.1		0.0	134.8	76.8
CASSCF							
	6-31G	126.5	0.0		0.0	126.5	57.2

For a better analysis, we will discuss the effect of the basis set separately from the dependency on the QM method and from the effects of the environment. Finally some considerations on the quantitative accuracy of present QM methodologies for the prediction of the electronic coupling will be reported with the comparison with available experimental data for the coupling in the BCL-BPH pair.

As a preliminary general comment, however, we note that in all pairs studied, the electronic coupling arises mainly from Coulomb interactions between the transition densities whatever is the QM method or the basis set used. This can be easily understood, as exchange and overlap (and eventually exchange-correlation) contributions are expected to be important only at very short interchromophoric separations. In the naphthalene dimer, for instance, only when diffuse functions are included through the 6-31+G(d) basis set, we obtain a non-negligible exchange contribution that amounts to 5% and 2% of the total coupling when CIS or SAC-CI transition densities are used, respectively, while for TD-B3LYP and CASSCF the contribution is less than 1%. In the stacked perylene pair, where a very short distance of 3.9 Å separates the two molecules, we find again the CIS method as the one giving rise to larger exchange contributions accounting for 1% of the total coupling, while for the other methods it is even smaller. For the PEB of the BCL-BPH systems, the exchange contribution is negligible.

Regarding the overlap term, its contribution is completely negligible in almost all cases, and only with the cc-

TABLE VIII. BCL-BPH dimer in vacuum: Coulomb, Hartree–Fock exchange, exchange-correlation, and overlap contributions to the total electronic couplings V along with the estimates obtained from the PDA $V^{\text{dip-dip}}$. Separation between the charge centers of 11.3 Å. All values are in cm^{-1}.

		$\mathbf{V}^{\text{Coul}}$	$\mathbf{V}^{\text{hfx}}$	$\mathbf{V}^{\text{xc}}$	$\mathbf{V}^{\text{ovlp}}$	$\mathbf{V}$	$\mathbf{V}^{\text{dip-dip}}$
ZINDO		306.4				306.4	485.1
CIS							
	6-31G	314.3	0.0		0.0	314.3	349.0
	6-31G(*d*)	325.1	−0.1		0.0	325.0	364.8
	cc-pVDZ	325.0	−0.1		0.0	324.9	366.6
	6-31+G(*d*)	332.4	−0.4		0.0	332.0	376.2
TD-B3LYP							
	6-31G	145.5	0.0	0.0	0.0	145.5	179.2
	6-31G(*d*)	146.7	0.0	0.0	0.0	146.7	181.9
	cc-pVDZ	145.5	0.0	0.0	0.0	145.5	181.8
	6-31+G(*d*)	153.3	0.0	−0.1	0.0	153.2	193.4
SAC-CI							
	6-31G	259.1	0.0		0.0	259.1	295.8
CASSCF							
	6-31G	212.6	0.0		0.0	212.6	226.5

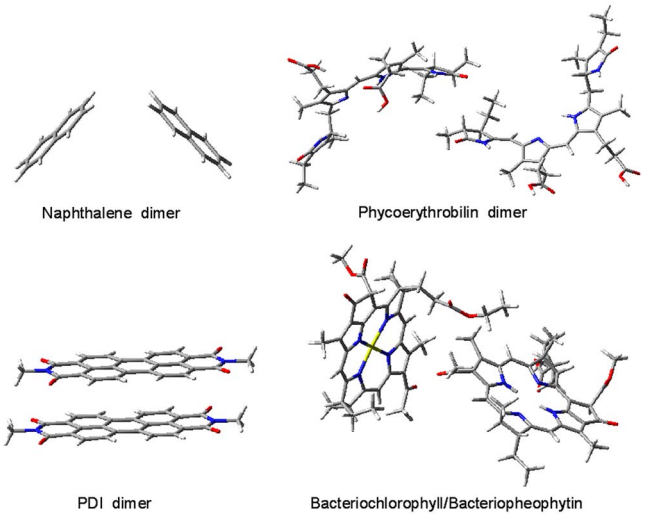

FIG. 1. (Color online) Structures of the chromophore pairs studied.

pVDZ basis set it amounts to ~1% of the total coupling in the naphthalene, perylene, and PEB pairs. On the other hand, the exchange-correlation term obtained with TD-B3LYP amounts to some units of cm^{-1} only when diffuse functions are included through the 6-31+G(*d*) basis set for the naphthalene and perylene systems, again although contributing less than 1% to the total.

Following these results, the following discussion on the effect of the QM method and basis set combination for the calculation of EET couplings will be mainly focused in the differences arising in the long-range Coulomb term, as all the other contributions are negligible for all the systems.

1. Basis set sensitivity

As expected from the results on transition dipoles reported in the previous section, the electronic coupling is quite robust with respect to changes in the basis set. In fact, if we consider a particular pair and a fixed QM level, the percent variation obtained when passing from the 6-31G basis set to 6-31G(*d*), 6-31+G(*d*), or cc-pVDZ is always 10% or lower. The only exception to this trend is represented by TD-B3LYP calculations on the PEB pair, in which the 6-31G basis set gives a ~30% smaller coupling with respect to the other basis sets. This fact arises as a consequence of the presence of a spurious charge-transfer state located at lower energy with respect to our state of interest in PEB, as already commented in the previous section. The degree of mixing of this state with our state of interest, which varies with basis set, leads to large changes in the transition dipoles, and consequently, in the electronic couplings.

If we exclude the particular case of TD-B3LYP calculations on the PEB pair, the largest basis set–induced change (10%) is found for the naphthalene dimer when passing from CIS/6-31G values to CIS/6-31+G(*d*), while for all the other chromophore pair/QM method combinations the change is always less than 8%. We note, however, that half of the change for the naphthalene/CIS case is originated by the large increase in the exchange term found with the introduction of diffuse functions, while only a 5% change is found on the Coulomb term. Interestingly, no clear trend is found in the electronic coupling with the enlargement of the basis set, i.e., the introduction of polarization and diffuse functions in some cases leads to an increase in the coupling, while in other cases it leads to a decrease. Such destructive or constructive additions to the coupling due to changes in the complex shape of the transition densities when the basis set is enlarged is expected to be mainly dictated by the orientation of the chromophores. However, we note that for the naphthalene pair we find opposite trends with respect to the other systems as the basis set is enlarged: CIS leads to smaller couplings while the other QM methods lead to increased ones as we pass from the 6-31G to 6-31G(*d*) and 6-31+G(*d*) basis sets. This suggests that the basis set effect on the coupling is a complex combination of orientational and QM effects.

2. QM method dependence

So far, we have seen that the changes in the basis set lead to variations smaller than 10% in the electronic coupling, but does this quantity substantially change depending on the QM method of calculation? If we consider CASSCF and SAC-CI couplings as benchmarks, it is clearly seen that CIS couplings are systematically overestimated in all cases, in agreement with the results obtained for the transition dipoles. The only exception is represented by the perylene dimer, where it is difficult to define a benchmark coupling estimate, as a substantially larger value (~23%) is found for CASSCF compared to SAC-CI. In this case, CIS couplings are ~7% smaller than CASSCF ones but again ~14% larger than SAC-CI estimates. For the naphthalene and PEB pairs, the overestimation amounts to ~20%–30%. Again, it is difficult to define a benchmark value for the BCL-BPH pair, as in this case we found a value for CASSCF, which is 18% smaller compared to the SAC-CI estimate. Nevertheless, CIS values are strongly overestimated, by ~20%–30% compared to SAC-CI, in line to what was found for other systems, and about ~48%–56% with respect to CASSCF. Taken together, these results show a quite constant relation between CIS and SAC-CI estimates, the former being 15%–30% larger. On the other hand, the choice of particular active spaces in CASSCF for each system could be the reason why the ratio between CIS and CASSCF results is less regular. In contrast to CIS, the TD-B3LYP method leads to underestimations of the electronic couplings of ~20% for the naphthalene system (when compared to both SAC-CI or CASSCF) and of ~37% (compared to CASSCF) or ~22% (compared to SAC-CI) for the perylene dimer. These latter results agree well with the calculations of Fückel *et al.*[20] who found ~15% smaller couplings for a perylene dyad when using transition densities obtained from TD-B3LYP compared to second-order approximate coupled cluster (CC2) calculations, which is a method comparable to SAC-CI. Regarding the photosynthetic PEB dimer, however, TD-B3LYP/6-31G values agree very well with those obtained using either CASSCF or SAC-CI with the same basis set. On the other hand, for the BCL-BPH pair we find that TD-B3LYP gives ~30%–40% smaller couplings compared to the more accurate CASSCF and SAC-CI methods. If we exclude the results for PEB (due to the problems in TD-B3LYP previ-

ously discussed), it is found that, in general, TD-B3LYP underestimates the electronic coupling by ~20%–40% compared to high-level methods such as SAC-CI and CASSCF.

A less regular behavior is found for the semiempirical ZINDO method. On the one hand, the transition dipoles calculated with ZINDO are, in general, similar to CIS ones except for the BCL-BPH pair, for which they are considerably larger. ZINDO transition dipoles are also substantially overestimated with respect to SAC-CI or CASSCF in all the four pairs; hence one could expect an overestimation of the couplings, as is the case when we apply the PDA approximation (see Tables V–VIII). On the other hand, ZINDO couplings strongly underestimate SAC-CI and CASSCF values for the naphthalene pair, representing approximately one-half of the CIS values, they agree quite well with SAC-CI or CASSCF for the perylene and PEB systems, and they overestimate the couplings for the BCL-BPH pair. We note here that in all cases small angular deviations are found between the transition dipole moments as obtained from the different QM methods, so that the differences in the predicted couplings cannot be explained by changes in the direction of the dipoles.

Finally, it is worth analyzing the differences found between our two "benchmark" methods, CASSCF and SAC-CI. Even if the philosophies underlying these two approaches are quite different, and, in fact, the estimates of transition energies significantly differ from one method to the other, these differences are significantly reduced for both transition dipoles and electronic couplings. For instance, SAC-CI couplings for the naphthalene and the PEB dimers only differ by 3%–6% with respect to CASSCF values. In the case of the stacked perylene pair, these differences are larger, amounting to ~20%, despite the fact that both approaches give similar values for the transition dipole. This can be understood by keeping in mind the short interchromophoric separation of 3.9 Å in this system, so here differences in the description of the transition densities between the two methods should be amplified in the calculation of the coupling. However, given that very similar transition dipoles are obtained from both methods, at larger separations the couplings obtained are expected to converge to a similar value. The largest difference between transition dipoles is found for the BCL-BPH pair, which translates into an electronic coupling 18% smaller obtained for CASSCF compared to the SAC-CI value.

Overall, these two methods are in much better agreement regarding the evaluation of the electronic coupling than when compared to any other approach used in this work; CIS and TD-B3LYP leading to quite systematical overestimations and underestimations of such a quantity, respectively, and ZINDO results being quite unpredictable.

To summarize, in Fig. 2 we report the mean signed and unsigned percent errors (MSPE,MUPE) of each method with respect to SAC-CI for both the QM and PDA couplings. The MUPE values indicate the systematic overestimation/underestimation of electronic couplings by the CIS and TD-B3LYP methods, while CASSCF agrees better on average with SAC-CI. In addition, we find that ZINDO results are difficult to assess on the basis of the calculated transition dipole strengths, given that the satisfactory agreement obtained for the QM values contrasts to the strong errors estimated by the PDA.

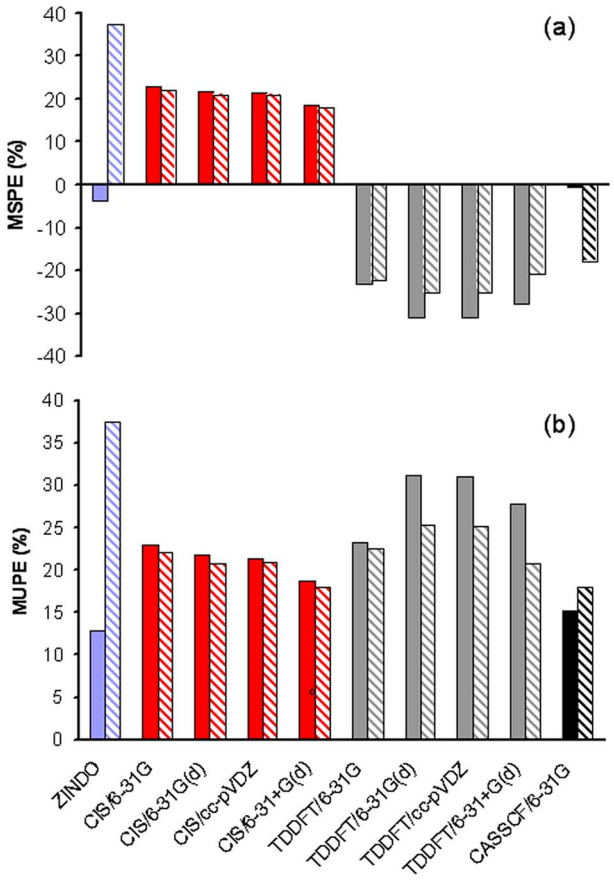

FIG. 2. (Color online) Mean signed percent variations (a) and mean unsigned percent variations (b) with respect to SAC-CI for both the QM (filled column) and PDA (striped column) couplings. SAC-CI reference values have been obtained using 6-31+G(*d*) for naphthalene, 6-31G(*d*) for PDI, and 6-31G for bilins and chlorophylls.

3. Environment effects

Finally, we discuss the sensitivity of the PCM medium effects in the coupling with respect to the choice of QM method. This analysis is restricted to those QM methods (ZINDO, CIS, and TD-DFT) for which the present implementation of EET couplings can include PCM effects; due to the weak sensitivity of the gas-phase couplings to the basis set, CIS and TD-B3LYP results for the PEB and BCL-BPH solvated systems will be limited to the 6-31G basis set only.

In Tables IX–XI we show the results obtained for the naphthalene dimer in *n*-hexane solution, for the perylene system in toluene, and for the two photosynthetic pairs in a protein environment, respectively.

As a first observation, we can see that for all calculations the presence of the dielectric environment induces an increase in the Coulomb term, in accord with the observed increases in the transition dipoles. The only case where there is a slight 2% decrease in this term occurs for the PEB pair at the ZINDO level. This implicit effect of the medium in the transition densities, and thus in the coupling, is, however, somewhat different depending on the QM method applied.

TABLE IX. Naphthalene dimer in *n*-hexane: Coulomb, explicit solvent, Hartree–Fock exchange, exchange-correlation, and overlap contributions to the total electronic coupling V and estimates from the PDA $V^{\text{dip-dip}}/n^2$, obtained using the transition dipoles calculated in condensed phase. The values in brackets refer to percent variations with respect to vacuum. All couplings are in cm^{-1}.

		$\mathbf{V}^{\text{Coul}}$	$\mathbf{V}^{\text{explicit}}$	$\mathbf{V}^{\text{hfx}}$	$\mathbf{V}^{\text{xc}}$	$\mathbf{V}^{\text{ovlp}}$	$\mathbf{V}$	$\mathbf{V}^{\text{dip-dip}}/\boldsymbol{n}^2$
ZINDO		738.8 (9)	−295.9				442.9 (−35)	611.2 (−44)
CIS								
	6-31G	1280.2 (7)	−373.2	−0.2		0.0	906.9 (−25)	659.1 (−42)
	6-31G(*d*)	1271.6 (7)	−371.2	−0.2		0.0	900.2 (−24)	655.6 (−41)
	cc-pVDZ	1307.9 (7)	−381.1	−0.7		−2.4	923.7 (−24)	673.6 (−41)
	6-31+G(*d*)	1268.9 (11)	−371.2	−31.8		0.0	865.8 (−20)	651.9 (−36)
TD-B3LYP								
	6-31G	804.2 (13)	−242.0	0.0	0.1	0.0	562.6 (−21)	426.9 (−38)
	6-31G(*d*)	792.6 (13)	−238.5	0.0	0.1	0.0	554.2 (−21)	421.0 (−38)
	cc-pVDZ	819.5 (14)	−264.1	0.0	0.1	−0.3	573.1 (−21)	435.2 (−38)
	6-31+G(*d*)	876.3 (13)	−262.0	−4.3	−6.4	0.1	603.7 (−21)	461.1 (−38)

We find that TD-B3LYP Coulomb terms are systematically enlarged compared to their CIS counterparts, with ZINDO estimates being somewhat between CIS and TD-B3LYP. For naphthalene, we find increases in this term ranging from 7% to 11% for CIS, while for TD-B3LYP 13%–14% increases are found. For perylene, the 12%–13% increase obtained with CIS can be compared to the much larger 23% value obtained with TD-B3LYP. Similarly, in the case of BCL-BPH pair we found a 20% increase in CIS and a 33% one with TD-B3LYP. The smallest change is obtained for the PEB pair, in which CIS gives a negligible change in the Coulomb term, while TD-B3LYP predicts a 7% increase.

Besides this implicit effect through the modification of the corresponding transition densities, the surrounding medium explicitly enters in the expression of the coupling through the V_{explicit} contribution, which describes the environment-mediated chromophore-chromophore interaction. As described in Sec. II, one can define a screening factor s [see Eq. (2)], which can be directly compared to Förster screening factor ($s_{\text{Förster}}=1/n^2$). As we showed recently,[15] this term is far from being a constant factor as assumed in Förster theory, as it greatly depends on the geometrical details (distance, shape, and orientation) of the particular system under scrutiny. The results obtained for the factor s in the various dimers are reported in Fig. 3 together with the Förster value.

In our calculations, we obtain very similar screening factors using either CIS or TD-B3LYP, while the ZINDO method systematically predicts lower values of s. For naphthalene, the CIS/TD-B3LYP $s=0.70-0.71$ estimates are much higher than the $s_{\text{Förster}}=0.53$ prediction in *n*-hexane. In a similar way, the $s=0.60-0.63$ estimates for the perylene dimer are much higher than the $s_{\text{Förster}}=0.45$ value predicted by Förster theory in toluene. Again, for the BCL-BPH pair we find a much larger value ($s=0.73$) using CIS/TD-B3LYP calculations than applying the Förster model ($s_{\text{Förster}}=0.50$). The best accord between our screening factor and Förster prediction is found for the PEB pair ($s=0.54-0.56$, $s_{\text{Förster}}=0.50$). This can be understood because in this case the two chromophores are farther away (of 17.1 Å) and it is well known that Förster theory is a good approximation at large distances. That means that for the PEB dimer, there is a more significant presence of the environment in between the two chromophores that more effectively screens their interactions compared to the other more closely spaced systems. These

TABLE X. PDI dimer in toluene: Coulomb, explicit solvent, Hartree–Fock exchange, exchange-correlation, and overlap contributions to the total electronic coupling V and the estimates from the PDA $V^{\text{dip-dip}}/n^2$ obtained using the transition dipoles calculated in condensed phase. The values in brackets refer to percent variations with respect to vacuum. All couplings are in cm^{-1}.

		$\mathbf{V}^{\text{Coul}}$	$\mathbf{V}^{\text{explicit}}$	$\mathbf{V}^{\text{hfx}}$	$\mathbf{V}^{\text{xc}}$	$\mathbf{V}^{\text{ovlp}}$	$\mathbf{V}$	$\mathbf{V}^{\text{dip-dip}}/\boldsymbol{n}^2$
ZINDO		1468.0 (18)	−699.6				768.4 (−38)	4180.6 (−48)
CIS								
	6-31G	1687.8 (12)	−629.7	14.7		0.0	1072.8 (−30)	3658.5 (−49)
	6-31G(*d*)	1617.7 (13)	−598.9	14.1		0.0	1032.8 (−29)	3464.8 (−49)
	cc-pVDZ	1587.1 (13)	−587.0	18.9		−0.2	1018.8 (−28)	3392.2 (−48)
	6-31+G(*d*)	1564.8 (12)	−587.2	13.2		0.1	990.7 (−30)	3419.5 (−48)
TD-B3LYP								
	6-31G	1254.9 (23)	−488.0	0.3	0.0	0.0	767.2 (−25)	3002.1 (−43)
	6-31G(*d*)	1201.2 (23)	−467.1	0.3	0.0	0.0	734.4 (−25)	2873.0 (−43)
	cc-pVDZ	1181.2 (23)	−459.3	0.4	−0.2	0.0	722.1 (−25)	2825.5 (−42)
	6-31+G(*d*)	1215.7 (23)	−481.2	−0.8	−2.0	0.0	731.7 (−26)	2998.6 (−42)

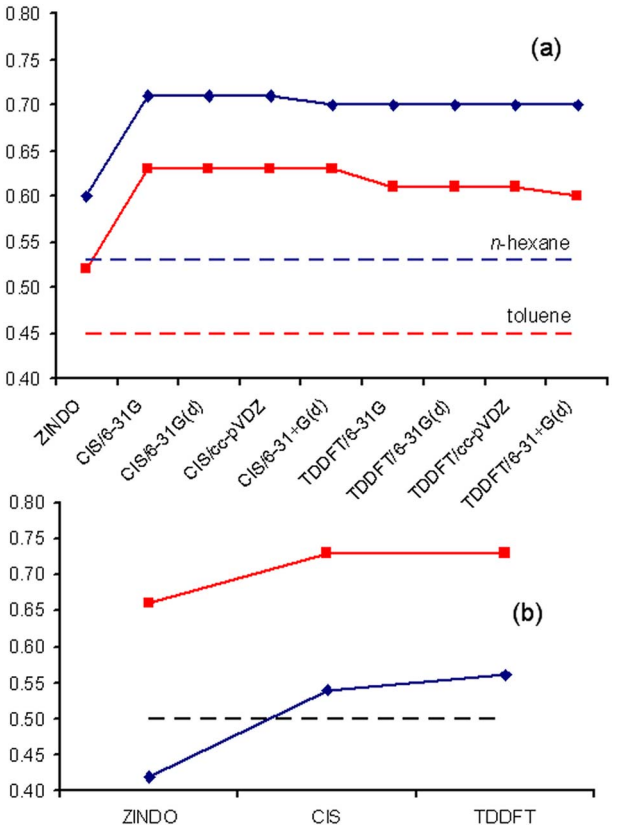

FIG. 3. (Color online) Screening factor s at different QM levels for (a) naphthalene dimer in n-hexane [blue (black) line with diamonds] and PDI dimer in toluene [red (black) line with squares] and (b) PEB 50/61D—PEB 50/61C [blue (black) line with diamonds] and the BCL-BPH dimers in protein [red (black) line with squares]. Förster values are reported as dashed lines.

results are in good agreement with the empirical distance-dependent screening function we have recently proposed for the evaluation of electronic couplings in photosynthetic antenna systems.[16]

Finally, we comment on the quantitative accuracy that can be expected in calculations of electronic couplings with currently available QM methods. Given the strong modulation of the EET coupling arising from the presence of the environment, the development of accurate QM methodologies for its prediction has to be accompanied by the development of equally reliable methods for the inclusion of environment effects that can be efficiently coupled to the QM calculations. Another problem consists in the difficulty to obtain accurate experimental estimates, which can be directly compared to theory; these, in fact, are often derived from EET rates and so they can be contaminated by different sources of error. A direct experimental measure of the coupling for rigid bridged model dyads has been reported from observed splittings in the dimer spectra,[21] but this is only possible if both dimer states are optically allowed. For this series of bridged naphthalene dimers, we have recently reported estimates within 20% error of the intramolecular EET couplings in n-hexane solution, obtained either by explicitly accounting for through-bond contributions[24] to the coupling or instead by deriving the coupling from the splitting of the dimer states in CIS "supermolecule" calculations,[12(b)] in both cases introducing solvent effects through the PCM model.

For intermolecular EETs, however, the accuracy of theoretical predictions is expected to be better than for intramolecular EETs, as we do not need to account for complex through-bond effects. Recently Fleming *et al.* have reported a direct experimental estimation of the electronic coupling between the BCL-BPH pair of the RC of the purple photosynthetic bacterium *Rhodobacter sphaeroides* we have considered in this study.[29] By using one-and two-color, three-pulse photon echo peak shift spectroscopy an experimental estimate of $170 \pm 30\ \mathrm{cm}^{-1}$ has been obtained. Our TD-B3LYP result in the protein environment, $140\ \mathrm{cm}^{-1}$, is within the error bar of the experimental estimate, while CIS or ZINDO methods substantially overestimate experiment. On the other hand, if we assume a protein effect (both implicit and explicit screening effects) in the range of what was obtained for ZINDO, CIS, or TD-B3LYP (from −18% to −4% change), SAC-CI couplings in solution would be in the range of $210-250\ \mathrm{cm}^{-1}$, while CASSCF ones in the range of $175-205\ \mathrm{cm}^{-1}$. We therefore find our most accurate TD-B3LYP, SAC-CI, or CASSCF results to range approximately from the lower bound to the upper bound of the experimental estimate. This comparison between calculated and experimental coupling gives us confidence in the idea that the dielectric permittivities we use here to simulate a protein environment through PCM are reasonable and support their use

TABLE XI. PEB 50/61D-PEB 50/61C and the BCL-BPH dimers in the protein environment: Coulomb, explicit solvent, Hartree–Fock exchange, exchange-correlation, and overlap contributions to the total electronic couplings V and estimates from the PDA $V^{\mathrm{dip\text{-}dip}}/n^2$ obtained using the transition dipoles calculated in condensed phase. All calculations are done with the 6-31G basis set. The values in brackets refer to percent variations with respect to vacuum. All couplings are in cm^{-1}.

	$\mathbf{V}^{\mathrm{Coul}}$	$\mathbf{V}^{\mathrm{explicit}}$	$\mathbf{V}^{\mathrm{hfx}}$	$\mathbf{V}^{\mathrm{xc}}$	$\mathbf{V}^{\mathrm{ovlp}}$	$\mathbf{V}$	$\mathbf{V}^{\mathrm{dip\text{-}dip}}/\boldsymbol{n}^2$
			PEB 50/61D - PEB 50/61 C				
ZINDO	129.7 (−2)	−75.8				53.9 (−59)	49.7 (−48)
CIS	169.3 (0)	−77.0	−0.1		0.0	92.2 (−46)	49.3 (−47)
TD-B3LYP	138.1 (7)	−60.5	0.0	−0.1	0.0	77.6 (−40)	36.9 (−41)
			BCL-BPH				
ZINDO	382.0 (25)	−130.4				251.6 (−18)	311.8 (−36)
CIS	378.1 (20)	−100.9	0.1		0.0	277.2 (−12)	223.1 (−36)
TD-B3LYP	192.8 (33)	−52.5	0.0	0.0	0.0	140.3 (−4)	127.0 (−29)

in our recent derivation of an empirical distance-dependent screening function to study EETs in photosynthetic antenna systems. Furthermore, this agreement suggests that QM methodologies for the electronic coupling are approaching their maturity toward efficient quantitative estimation of electronic couplings.

IV. SUMMARY

We have presented a comparative study on the influence of the QM method (including basis set) on the evaluation of transition energies, densities and dipoles, and EET electronic couplings for a series of chromophores (and the corresponding donor-acceptor pairs) typically found in organic electro-optical devices and photosynthetic systems. On these systems we have applied five different QM levels of description of increasing accuracy (ZINDO, CIS, TD-DFT, CASSCF, and SAC-CI). In addition, we have tested the effects of a surrounding environment (either mimicking a solvent or a protein matrix) on excitation energies, transition dipoles, and electronic couplings through the PCM description.

As expected, the comparison with experiments on excitation energies has confirmed the importance of using extended basis sets as well as the superiority of SAC-CI and CASPT2 with respect to the other methods, even if TD-B3LYP has also shown a very good behavior for most of the systems. In any case, excitation energies have been found to vary strongly with the QM method. In contrast, solvent shifts as well as transition dipole moments have shown to be much less sensitive to the particular level of theory, and even less with respect to the basis set.

Moving to EET parameters, the electronic coupling is found to be more stable than the excitation energies with respect to the QM level of description and to have little dependence on the basis set. In particular, a good agreement has been found between the SAC-CI and CASSCF calculations, whereas CIS and TD-B3LYP typically lead to couplings increased or reduced, respectively, by more than 20% with respect to SAC-CI. Finally, a less regular behavior is found for ZINDO, which strongly overestimates transition dipoles leading to subsequent increases in the couplings obtained from the PDA, whereas couplings computed from transition densities can be either underestimated or overestimated depending on the particular pair of molecules considered.

With regard to solvent effects on the couplings, we find that the well-known Förster factor $1/n^2$ significantly overestimates the screening of the EET couplings compared to the more realistic PCM estimates, in which a molecular-shaped cavity enclosing the chromophores is used to represent the environment polarization. This is particularly evident in the more closely packed naphthalene, PDI, and BCL-BPH pairs. Here, the EET rates (proportional to V^2) in the PCM case are 1.5–2.0 times larger than it would be predicted using a simple $1/n^2$ screening model. In addition to the screening, a PCM environment affects also the transition densities, and this can lead to an increase of the coupling through a larger Coulomb term. In all the systems studied (with the exception of the PEB pair), PCM effects on transition densities lead to 10%–30% increases in the couplings, thus counteracting screening effects and leading to even larger predicted EET rates.

Overall, our results suggest that estimates of electronic couplings are much less affected by the choice of the QM level of theory than excitation energies are. We conclude that reasonable estimates can be obtained using moderate basis sets and inexpensive methods such as CIS or TD-DFT when appropriately coupled to realistic solvation models such as PCM. However, improved quantitative accuracy requires some empirical scaling procedure to account for systematic errors observed when compared to high-level correlated methods such as SAC-CI and CASSCF. We finally note that care has to be taken when using TD-DFT methods, as possible mixings of the state of interest with spurious low-lying states can introduce strong variations in the electronic coupling. This problem, however, is expected to be largely alleviated by recent developments of long-range corrected exchange-correlation functionals.

ACKNOWLEDGMENTS

I.F.G. acknowledges the Junta de Extremadura and the European Social Fund for financial support.

[1] G. R. Fleming and G. D. Scholes, Nature (London) **431**, 256 (2004).
[2] Y. Kuramochi, A. Satake, M. Itou, K. Ogawa, Y. Araki, O. Ito, and Y. Kobuke, Chem.-Eur. J. **14**, 2827 (2008).
[3] T. M. Swager, Acc. Chem. Res. **31**, 201 (1998).
[4] J.-I. Lee, I.-N. Kang, D.-H. Hwang, H.-K. Shim, S.-C. Jeoung, and D. Kim, Chem. Mater. **8**, 1925 (1996).
[5] S. Weiss, Nat. Struct. Biol. **7**, 724 (2000).
[6] C. Curutchet, in *Solvent Effects in Photoinduced Energy and Electron Transfers: the Electronic Coupling*, Continuum Solvation Models in Chemistry, edited by B. Mennucci and R. Cammi (Wiley, New York, 2008).
[7] T. Förster, Ann. Phys. (Leipzig) **2**, 55 (1948), translated in *Biological Physics*, edited by E. Mielczarek, R. S. Knox, and E. Greenbaum (American Institute of Physics, New York, 1993), pp. 148–160.
[8] B. P. Krueger, G. D. Scholes, R. Jimenez, and G. R. Fleming, J. Phys. Chem. B **102**, 2284 (1998); B. P. Krueger, G. D. Scholes, and G. R. Fleming, *ibid.* **102**, 5378 (1998); **102**, 9603 (1998).
[9] G. D. Scholes, X. J. Jordanides, and G. R. Fleming, J. Phys. Chem. B **105**, 1640 (2001); J. S. Frähmcke and P. J. Walla, Chem. Phys. Lett. **430**, 397 (2006); J. M. Jean and B. P. Krueger, J. Phys. Chem. B **110**, 2899 (2006); D. Zigmantas, E. L. Read, T. Mancal, T. Brixner, A. T. Gardiner, R. J. Cogdell, and G. R. Fleming, Proc. Natl. Acad. Sci. U.S.A. **103**, 12672 (2006); E. Dolghih, A. E. Roitberg, and J. L. Krause, J. Photochem. Photobiol., A **190**, 321 (2007); A. Czader and E. R. Bittner, J. Chem. Phys. **128**, 035101 (2008).
[10] S. Tretiak, W. M. Zhang, V. Chernyak, and S. Mukamel, Proc. Natl. Acad. Sci. U.S.A. **96**, 13003 (1999); S. Tretiak and S. Mukamel, Chem. Rev. (Washington, D.C.) **102**, 3171 (2002).
[11] C.-P. Hsu, G. R. Fleming, M. Head-Gordon, and T. J. Head-Gordon, Chem. Phys. **114**, 3065 (2001).
[12] (a) M. F. Iozzi, B. Mennucci, J. Tomasi, and R. Cammi, J. Chem. Phys. **120**, 7029 (2004); (b) C. Curutchet and B. Mennucci, J. Am. Chem. Soc. **127**, 16733 (2005).
[13] C. Curutchet, R. Cammi, B. Mennucci, and S. Corni, J. Chem. Phys. **125**, 054710 (2006).
[14] B. Mennucci, J. Tomasi, and R. Cammi, Phys. Rev. B **70**, 205212 (2004).
[15] C. Curutchet, B. Mennucci, G. D. Scholes, and D. Beljonne, J. Phys. Chem. B **112**, 3759 (2008).
[16] G. D. Scholes, C. Curutchet, B. Mennucci, R. Cammi, and J. Tomasi, J. Phys. Chem. B **111**, 6978 (2007); C. Curutchet, G. D. Scholes,

B. Mennucci, and R. Cammi, *ibid.* **111**, 13253 (2007).
[17] V. M. Huxter and G. D. Scholes, in *Excitation Energy Transfer and the Role of the Refractive Index*, Continuum Solvation Models in Chemistry, edited by B. Mennucci and R. Cammi (Wiley, New York, 2008).
[18] J. Tomasi, B. Mennucci, and R. Cammi, Chem. Rev. (Washington, D.C.) **105**, 2999 (2005).
[19] G. D. Scholes and G. R. Fleming, Adv. Chem. Phys. **132**, 57 (2005).
[20] B. Fückel, A. Köhn, M. E. Harding, G. Diezemann, H. Hinze, T. Basché, and J. Gauss, J. Chem. Phys. **128**, 074505 (2008).
[21] G. D. Scholes, K. P. Ghiggino, A. M. Oliver, and M. N. Paddon-Row, J. Am. Chem. Soc. **115**, 4345 (1993).
[22] A. H. A. Clayton, G. D. Scholes, K. P. Ghiggino, and M. N. Paddon-Row, J. Phys. Chem. **100**, 10912 (1996).
[23] S. Tretiak, W. M. Zhang, V. Chernyak, and S. Mukamel, Proc. Natl. Acad. Sci. U.S.A. **96**, 13003 (1999).
[24] V. Russo, C. Curutchet, and B. Mennucci, J. Phys. Chem. B **111**, 853 (2007).
[25] R. Métivier, F. Nolde, K. Müllen, and T. Basché, Phys. Rev. Lett. **98**, 047802 (2007).
[26] A. B. Doust, C. N. J. Marai, S. J. Harrop, K. E. Wilk, P. M. G. Curmi, and G. D. Scholes, J. Mol. Biol. **344**, 135 (2004).
[27] U. Ermler, G. Fritzsh, S. K. Buchanan, and H. Michel, Structure (London) **2**, 925 (1994).
[28] D. Y. Parkinson, H. Lee, and G. R. Fleming, J. Phys. Chem. B **111**, 7449 (2007).
[29] M. C. Zerner, J. Chem. Phys. **62**, 2788 (1975); M. C. Zerner, Rev. Comput. Chem. **2**, 313 (1991).
[30] J. B. Foresman, M. Head-Gordon, J. A. Pople, and M. J. Frisch, J. Phys. Chem. **96**, 135 (1992).
[31] M. E. Casida, in *Recent Advances in Density Functional Methods*, edited by D. P. Chong (World Scientific, Singapore, 1995), Pt. 1; E. U. K. Gross, J. F. Dobson, and M. Petersilka, in *Density Functional Theory II*, edited by R. F. Nalewajski (Springer, Heidelberg, 1996).
[32] M. Ehara, M. Ishida, K. Toyota, and H. Nakatsuji, in *Reviews in Modern Quantum Chemistry*, edited by K. D. Sen (World Scientific, Singapore, 2002), p. 293.
[33] B. O. Roos, P. R. Taylor, and P. E. M. Siegbahn, Chem. Phys. **48**, 157 (1980).
[34] K. Andersson, P.-Å. Malmqvist, B. O. Roos, A. J. Sadlej, and K. Wolinski, J. Phys. Chem. **94**, 5483 (1990); K. Andersson, P.-Å. Malmqvist, and B. O. Roos, J. Chem. Phys. **96**, 1218 (1992).
[35] X. J. Jordanides, M. J. Lang, X. Y. Song, and G. R. Fleming, J. Phys. Chem. B **103**, 7995 (1999).
[36] A. K. Rappé, C. J. Casewit, K. S. Colwell, W. A. Goddard III, and W. M. Skiff, J. Am. Chem. Soc. **114**, 10024 (1992).
[37] M. J. Frisch, G. W. Trucks, H. B. Schlegel *et al.*, GAUSSIAN 03, Revision C.02, Gaussian, Inc., Wallingford CT, 2004.
[38] E. Hadicke, F. Graser, Acta Crystallogr., Sect. C: Cryst. Struct. Commun. **42**, 189 (1986).
[39] K. Andersson, M. Barysz, A. Bernhardsson *et al.*, MOLCAS Version 6, University of Lund, Lund, Sweden, 2006.
[40] G. A. George and G. C. Morris, J. Mol. Spectrosc. **26**, 67 (1968).
[41] H. B. Klevens and J. R. Platts, J. Chem. Phys. **17**, 470 (1949).
[42] Y. Li, J. Wang, and X. Xu, J. Comput. Chem. **28**, 1658 (2007).
[43] M. Schreiber, M. R. Silva-Junior, S. P. A. Sauer, and W. Thiel, J. Chem. Phys. **128**, 134110 (2008).
[44] B. Fückel, G. Hinze, G. Diezemann, F. Nolde, K. Müllen, J. Gauss, and T. Basché, J. Chem. Phys. **125**, 144903 (2006).
[45] A. B. Doust, K. E. Wilk, P. M. G. Curmi, and G. D. Scholes, J. Photochem. Photobiol., A **184**, 1 (2006).
[46] R. J. Magyar and S. Tretiak, J. Chem. Theory Comput. **3**, 976 (2007).
[47] O. A. Borg and B. Durbeel, J. Phys. Chem. B **111**, 11554 (2007).
[48] J. Hasegawa, M. Isshiki, K. Fujimoto, and H. Nakatsuji, Chem. Phys. Lett. **410**, 90 (2005).
[49] J. Wan, X. Xu, Y. Ren, and G. Yang, J. Phys. Chem. B **109**, 11088 (2005).
[50] C. Zazza, N. Sanna, and M. Aschi, J. Phys. Chem. B **111**, 5596 (2007).
[51] D. Y. Parkirson, H. Lee, and G. R. Fleming, J. Phys. Chem. B **111**, 7449 (2007).
[52] J. Hasegawa and H. Nakatsuji, Chem. Lett. **34**, 1242 (2005).
[53] M. Rubio, B. Roos, L. Serrano-Andrés, and M. Merchán, J. Chem. Phys. **110**, 7202 (1999).